Pseudoresonance mechanism of all-optical frequency-standard operation

G. Kazakov,[1] B. Matisov,[1] I. Mazets,[2] G. Mileti,[3] and J. Delporte[4]
[1]*St. Petersburg State Polytechnic University, St. Petersburg, 195251, Russia*
[2]*A.F. Ioffe Physics-Technical Institute, St. Petersburg 194021, Russia*
[3]*Observatoire Cantonal Neuchâtel, 2000 Neuchâtel, Switzerland*
[4]*Centre National d'Etudes Spatiales, 31401 Toulouse, France*
(Received 7 July 2005; published 21 December 2005)

We propose an approach to all-optical frequency standard design, based on a counterintuitive combination of the coherent population trapping effect and signal discrimination at the maximum of absorption for the probe radiation. The short-term stability of such a standard can achieve the level of $10^{-14}/\sqrt{\tau}$. The physics beyond this approach is a dark resonance splitting caused by the interaction of the nuclear magnetic moment with the external magnetic field.

DOI: 10.1103/PhysRevA.72.063408 PACS number(s): 32.80.Bx, 06.30.Ft, 42.50.Gy

The unit of time in the Système International (the second) is defined via the period of the transition between the hyperfine (HF) components of the ground state of the ^{133}Cs atom (in the limit of vanishing external perturbations). Secondary standards may use other elements (alkali metals, hydrogen). The operation of a frequency standard is provided by locking a microwave signal produced by a quartz crystal oscillator to a resonance on the transition between the working levels [1], i.e., the Zeeman components of the HF structure with zero projection of the total angular momentum. Such a choice of the working levels is dictated by the absence of the linear Zeeman shift. The resonance can be excited by direct microwave transition or by two-photon Raman transition. The latter option provides the basis for all-optical frequency standards [2–10] where the setup includes no microwave cavities, but electro-optical modulation of the laser beam, phase locking of two lasers, or direct modulation of the diode laser current are used instead.

If the interaction time of an atom with the laser field exceeds few optical pumping cycles then the coherent population trapping (CPT) sets in, giving rise to the so-called dark resonance [11,12]. The physical reason for the CPT is an optical pumping of atoms into a coherent superposition of the two ground state sublevels, which is immune to excitation by the frequency-split laser radiation. The CPT leads to a decrease of absorption of the laser light. However, if the Raman detuning (the difference between the frequency splitting of the two-component laser radiation and the transition frequency between the two ground state sublevels) exceeds the dark resonance width (what can be as a small as a few dozen Hz [7,13]), the CPT atomic state is destroyed, and the usual value of the laser radiation absorption is restored.

Keeping the frequency of a generator that provides laser frequency splitting coincident with the position of the dark resonance on the working transition is the physical mechanism of the frequency standardization by optical means.

In the present paper we propose a different, quite counterintuitive technique. No specific resonance on the working transition is excited. Instead, its frequency is identified as the position of maximum absorption between the two side dark resonances involving magnetically sensitive Raman transitions.

Before proceeding further, we have to recall some basic ideas from the theory of the CPT in systems with a closed-loop interaction contour [14]. An example of such a system is given in Fig. 1.

The reason why the σ^+/σ^--configuration of the laser radiation polarizations is used, instead of simply applying σ^+-polarized light only, is the adverse influence of the states with the maximum projection of the angular momentum ("pockets"), where most of the atoms are accumulated, thus drastically reducing the dark resonance amplitude and, hence, worsening the standard's performance. Pumping of the atoms out of pockets and returning them into the fraction of the atomic ensemble participating in the signal formation is, in principle, possible, but requires quite sophisticated techniques [9].

Consider the pair of the ground (g) state sublevels, $|F_g=F, m_g=m\rangle$ and $|F_g=F+1, m_g=m\rangle$, each of them resonantly coupled to the first excited (e) state sublevels $|F_e=F, m_e=m+1\rangle$ and $|F_e=F, m_e=m-1\rangle$ (or $|F_e=F+1, m_e=m+1\rangle$ and $|F_e=F+1, m_e=m-1\rangle$), thus forming the so-called double Λ closed loop interaction contour. Here F is the total angular momentum of the given HF component and m is the angular momentum projection to the quantization axis. The interac-

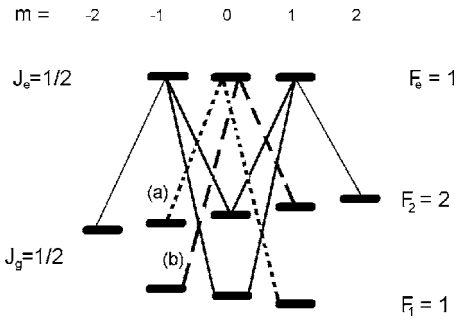

FIG. 1. Scheme of optically-induced transitions in the ^{87}Rb atom, case of $F_e=1$. "Closed loop" involving the working (0-0) transition *is* shown by bold solid black lines. Additional Λ schemes are shown by (a) dotted lines (the pairs of ground state Zeeman sublevels $|F_g=1, m=+1\rangle$, $|F_g=2, m=-1\rangle$ being involved), and (b) dashed lines ($|F_g=1, m=-1\rangle$, $|F_g=2, m=+1\rangle$ being involved).

tion matrix element for the transition $|F_g,m_g\rangle \leftrightarrow |F_e,m_e\rangle$ is

$$\langle F_g,m_g|\hat{V}|F_e,m_e\rangle = -\langle F_g,m_g|\hat{d}_q|F_e,m_e\rangle E_{F_g,F_e,q}, \qquad (1)$$

where $E_{F_g,F_e,q}$ is the complex amplitude of the laser field resonant to the given transition, $q=m_e-m_g$ denotes the cyclic component of the polarization unit vector, and the electric dipole element can be represented, according to the Wigner-Eckart theorem [15] as

$$\langle F_g,m_g|\hat{d}_q|F_e,m_e\rangle = (-1)^{F_g+J_e+I-1}\sqrt{2F_g+1} \times C^{F_e m_e}_{F_g m_g 1 q} \begin{Bmatrix} J_g & I & F_g \\ F_e & 1 & J_e \end{Bmatrix} \langle J_g||\hat{d}||J_e\rangle, \qquad (2)$$

where $J_{g(e)}$ is the electronic angular momentum of the ground (excited) state, I is the nuclear spin, $C^{F_e m_e}_{F_g m_g 1 q}$ is the Clebsh-Gordan coefficient,

$$\begin{Bmatrix} J_g & I & F_g \\ F_e & 1 & J_e \end{Bmatrix}$$

is the $6j$ symbol, and $\langle J_g||\hat{d}||J_e\rangle$ is the reduced matrix element of the dipole moment.

Let us consider the two Λ schemes produced by the laser radiation with σ^+ and σ^- polarizations separately. Let us introduce the corresponding Rabi frequencies as $V_{1,\pm}=\langle F_g=F,m|\hat{V}|F_e,m\pm 1\rangle$ and $V_{2,\pm}=\langle F_g=F+1,m|\hat{V}|F_e,m\pm 1\rangle$. The two corresponding CPT states, $|\mathrm{CPT}_+\rangle$ and $|\mathrm{CPT}_-\rangle$, can be identified as

$$|\mathrm{CPT}_\pm\rangle = \frac{V_{2,\pm}|F_g=F,m\rangle - V_{1,\pm}|F_g=F+1,m\rangle}{\sqrt{V_{1,\pm}^2+V_{2,\pm}^2}}. \qquad (3)$$

Let ς be a parameter defined via the relation

$$\frac{V_{2,+}}{V_{1,+}} = \varsigma\frac{V_{2,-}}{V_{1,-}}. \qquad (4)$$

If the amplitude and phase conditions [14,16] for the complex interaction matrix elements are satisfied, i.e., $\varsigma=+1$, then the two states defined by Eq. (3) coincide, and we get perfect CPT in the double Λ scheme. Then, if we scan the Raman detuning across the resonance, the dark resonance in the absorption spectrum appears [17]. In the contrary, if $\varsigma=-1$ then $|\mathrm{CPT}_+\rangle$ is the state corresponding to maximally enhanced absorption of the σ^- -polarized radiation, and *vice versa*. It makes CPT in such a double Λ scheme impossible. A simple but a bit lengthy analysis shows that no structure appears in the absorption spectrum near the resonance, *if no other ground state sublevels are taken into account*.

Unfortunately, satisfying the condition $\varsigma=+1$ implies sophisticated experimental techniques. Indeed, if all of the four components of the laser radiation, different in polarization and frequency, are obtained from the same input light beam by electro-optical modulator without specific precautions, one gets $E_{F,F_e,+1}/E_{F+1,F_e,+1}=E_{F,F_e,-1}/E_{F+1,F_e,-1}$. Due to the general property of Clebsh-Gordan coefficients [15], we always get for the working transition

$$\langle F,0|\hat{d}|F_e,+1\rangle/\langle F+1,0|\hat{d}|F_e,+1\rangle = -\langle F,0|\hat{d}|F_e,-1\rangle/\langle F+1,0|\hat{d}|F_e,-1\rangle \qquad (5)$$

that results in $\varsigma=-1$. Therefore one has to introduce a π phase shift to the σ^- component of the laser radiation, with respect to the σ^+ one. One solution, implemented by the NIST group [8,18], is based on counterpropagating configuration of σ^+-and σ^- polarized beams. In this case, the CPT condition $\varsigma=+1$ is satisfied in periodically located spatial regions, which are quite narrow (much less than a quarter of the HF transition wavelength). It limits the cell size to $\sim$1 mm. Dark resonances in such a miniaturized cell are quite broad, and the corresponding short-term stability is significantly reduced in comparison with that of a standard employing a cell of a size of about few cm. Recently high-contrast dark resonance has been demonstrated using the so-called "push-pull" technique [19,20], where a set of $\lambda/4$ plates, polarization-sensitive beam splitters and reflectors provides the necessary phase shift in the c.w. regime. Note that the amplitude modulation of the laser radiation was used in the experiments [19,20], although the authors of Refs. [19,20] mention that for low buffer gas pressures frequency modulation works as well. The "lin $\perp$ lin" technique developed by Zanon *et al.* [21] realizes a similar idea in time-domain (Ramsey) spectroscopy, using two phase-locked lasers. The setups of Refs. [19–21] are quite good for high-precision *laboratory* frequency standards. However, it is quite desirable to design a standard, which will be simpler in construction, easier to handle and, therefore, more suitable for operation on board of a satellite or in other mobile applications. In the present paper we propose a relevant approach.

We have obtained an intriguing result: the "adverse" condition $\varsigma=-1$ itself, holding for $m=0$, does not prevent precise spectroscopic identification of the working transition frequency and locking to it a quartz generator. The key factor here is the influence of the other Zeeman sublevels of the HF structure of the ground state. For the sake of definiteness, let us consider gas of ^{87}Rb atoms placed in a homogeneous magnetic field **H**. A linearly polarized laser radiation propagates along **H**. Its carrier frequency and modulation frequency are chosen so that the $F_g=1\leftrightarrow F_e=1$ and $F_g=2\leftrightarrow F_e=1$ components of the D_1 line are excited. Being projected to the quantization axis defined by the magnetic field, the linear polarization is represented by the coherent superposition of σ^+ and σ^- polarizations, see Fig. 1. Since there is no delay line for the σ^+-polarized component, we have $\varsigma=-1$ for $m=0$, and the corresponding double Λ scheme (shown by bold lines in Fig. 1) exhibits no CPT resonance. However, there are two additional Λ schemes, corresponding to quadrupole ($|\Delta m|=2$) two-photon transitions and involving the pairs of Zeeman sublevels $\{|F_g=1,m=+1\rangle, |F_g=2,m=-1\rangle\}$, indicated by the label (a) in Fig. 1, and $\{|F_g=1,m=-1\rangle, |F_g=2,m=+1\rangle\}$, indicated by the label (b) in Fig. 1. The distances between these ground state Zeeman sublevels in the weak magnetic field H are [1]

$$\omega_{a,b} = \omega_{hfs} \pm \frac{2g_I\mu_N}{\hbar}H + \frac{3g_J^2\mu_B^2}{8\omega_{hfs}\hbar^2}H^2, \qquad (6)$$

where ω_{hfs} is the hyperfine splitting frequency of the ground state HF components in the absence of the magnetic field,

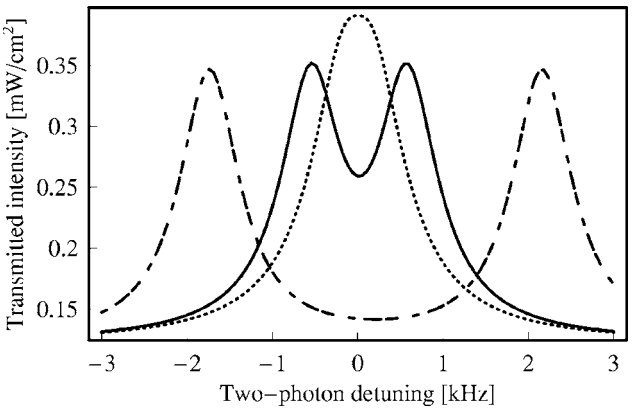

FIG. 2. Transmission spectrum of the cell with the parameters specified in the text. Incident radiation intensity $U_0=0.5$ mW/cm^2. The excitation scheme is shown in Fig. 1. The dotted line corresponds to $H=0.05$ G, the solid line corresponds to $H=0.2$ G, and the dotted-dashed line corresponds to $H=0.7$ G.

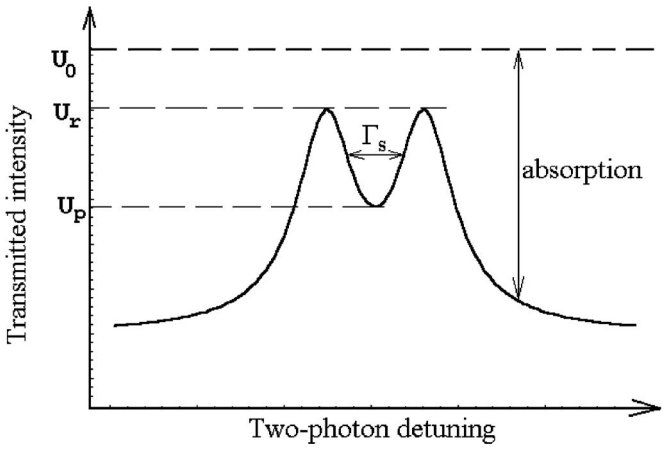

FIG. 3. Sketch of the pseudoresonance structure indicating the relevant intensity parameters and the full width Γ_s.

$\mu_B=e\hbar/(2m_ec)$ is the Bohr magneton, $\mu_N=e\hbar/(2m_pc)$ is the nuclear magneton, $g_I=\mu/\mu_N$ is the nuclear Lande factor, g_J is the electronic Lande factor, and μ is the magnetic momentum of atomic nucleus. The positive sign of the second term in the right-hand side of Eq. (6) corresponds to the Λ scheme denoted in Fig. 1 (a), the negative sign corresponds to the scheme Fig. 1(b). Recently it has been shown theoretically and proven experimentally [22] that such a "lin ∥ lin" excitation sceme gives rise to dark resonances of unprecedentedly high contrast, which is very promising for optical frequency standard design.

But not only high contrast of the dark resonances makes this scheme practically important. Note that one may erroneously treat these side dark resonances as magnetically insensitive in the linear approximation, if one does not take into account the magnetic moment of the nucleus, since the linear Zeeman shifts due to the electronic magnetic moment for each state in the pair $|F_g=1, m=\pm 1\rangle$, $|F_g=2, m=\mp 1\rangle$ are the same. The observation of the splitting of dark resonances due to the interaction of nuclear spins with external magnetic field was first reported, to the best of our knowledge, in Ref. [23] for Cs atoms, and recently [22] for ^{87}Rb atoms. In Eq. (6) we retain, for the sake of generality, the second-order Zeeman effect terms.

Therefore, the magnetic field shifts the positions of the corresponding dark resonances close to the working transition. The two dark resonances are symmetric (to the second-order Zeeman effect) with respect to the position of the $|F_g=1,m=0\rangle \leftrightarrow |F_g=2,m=0\rangle$ working transition. If the magnetic field shift is small (in comparison with the dark resonance width), the two dark resonances are not resolved, see Fig. 2, the dotted curve. For intermediate values of H they are resolved partially, thus forming a minimum in the transmission spectrum exactly between them, see Fig. 2, the solid curve. The position of this minimum coincides with the frequency of the $|F_g=1,m=0\rangle \leftrightarrow |F_g=2,m=0\rangle$ transition and can be implemented in a discriminator of an all-optical frequency standard. Such a structure formed between two maxima in the transmission spectrum can be called a *pseudoresonance*. The minimum width of the pseudoresonance is of the order of the dark resonance width. Further increase of H makes the two dark resonances fully resolved. As a result, the bottom of the pseudoresonance dip becomes flat, which is unsuitable for the frequency standardization purposes, see Fig. 2, the dotted-dashed curve. The second-order Zeeman shift of the pseudoresonance is of order of the same shift for the working transition.

Conventional dark resonance can be characterized by the amplitude, the width, and the contrast. Let us introduce the similar parameters for the pseudoresonance (the description of the parameters is illustrated by Fig. 3). We define the amplitude $A=U_r-U_p$ as the difference between the transmitted intensity U_r at the maximum of transmission and transmitted intensity U_p at the pseudoresonance center. The contrast $C=A/(U_0-U_p)$ is the ratio of the amplitude A to the intensity U_0-U_p absorbed in the cell under the pseudoresonance conditions.

The light shift of the pseudoresonance position is the same as that of each of the two sided dark resonances [24,25].

Note that the $F_e=2$ component of the ^{87}Rb D_1 line cannot be used for pseudoresonance creation, since in this case the states $|F_e=2, m=\pm 2\rangle$ are excited thus turning the relevant Λ schemes into W-type schemes, in which CPT is not possible [11]. The D_2 line is also unsuitable because of the small magnitude of the HF splitting of the $5\,^2P^o_{3/2}$ excited state and, hence, strong overlapping of Doppler contours of optical transitions to different HF components of the excited state.

We performed numerical simulations of linearly polarized, two-component laser light propagation through a ^{87}Rb gas cell with the following parameters: radius $R_c=1$ cm, length $L_c=2.5$ cm, number density $n=1.1\times 10^{11}$ cm^{-3} ($T=327$ K), and the diffusion coefficient for ^{87}Rb atoms $D=20$ cm^2/s corresponding to the buffer gas (N_2) pressure $=15$ Torr (such a pressure is chosen to provide a quenching of the excited state and thus diminish rescattering of photons). The relaxation rate Γ of ground state coherences in such a cell is dominated by wall collisions [1] and can be estimated as $\Gamma \approx 300$ s^{-1}. The density matrix formalism taking into account the whole manifold of the states, i.e., all Zeeman sublevels of all the involved hyperfine components

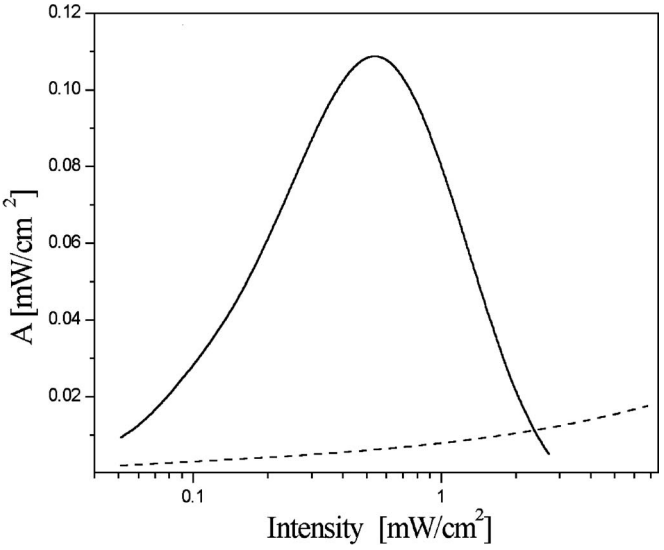

FIG. 4. Amplitude of the resonance in the cases of conventional dark resonance in the σ^+ configuration (dashed line) and of the pseudoresonance (solid line). The magnetic field $H=0.2$ G.

of the ground and excited states, was applied. The results are shown in Figs. 2 and 4–7. Apparently, the width of the absorption peak of about 0.7 kHz is achievable simultaneously with the contrast $C\sim 30\%$ (Fig. 2).

The amplitude A, the amplitude-to-width ratio A/Γ_s, and the contrast C of the pseudoresonance and of the dark resonance for the σ^+-excitation scheme are displayed in Figs. 4–6, respectively, as functions of the intensity of the incident laser radiation.

In Fig. 7 we plot the stability σ_y of the standard based on the *pseudoresonance* discrimination method versus the incident radiation intensity for different values of external magnetic fields [1]:

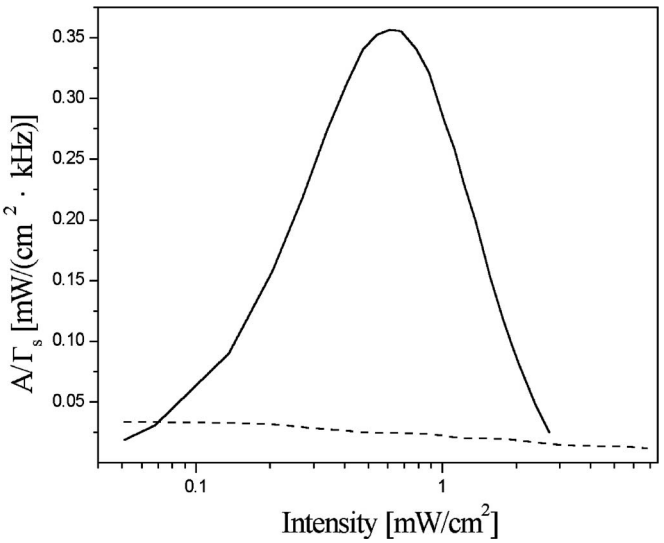

FIG. 5. Amplitude-to-width ratio of the resonance in the cases of conventional dark resonance in the σ^+ configuration (dashed line) and of the pseudoresonance (solid line). The magnetic field $H=0.2$ G.

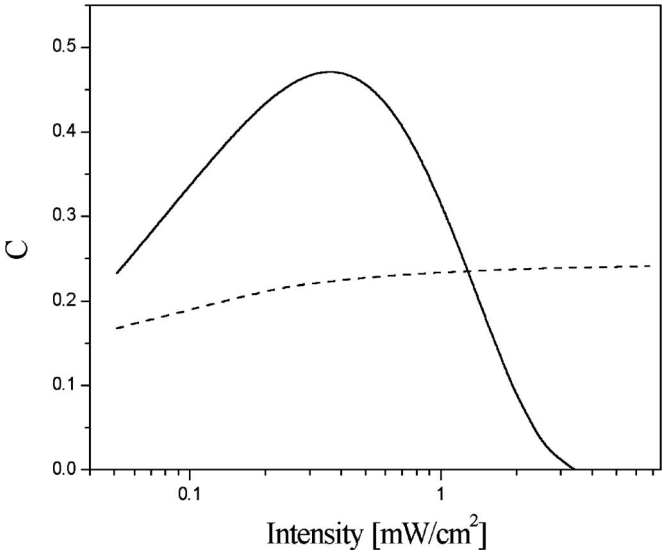

FIG. 6. Contrast (dimensionless) of the resonance in the cases of conventional dark resonance in the σ^+ configuration (dashed line) and of the pseudoresonance (solid line). The magnetic field $H=0.2$ G.

$$\sigma_y \approx \left(\omega_{hfs} |S''(0)| W f(\Theta) \sqrt{\frac{P\tau}{\hbar\omega_0}} \right)^{-1}, \qquad (7)$$

where $P=U_0\mathcal{F}$ is the total laser radiation power, U_0 being the intensity at the cell input, and $\mathcal{F}$ being the effective beam cross-section area (in our simulations we assume that the laser beam is wide enough to provide $\mathcal{F}\approx\pi R_c^2$), τ is the integration time, ω_0 is the D_1-line resonance frequency, $S''(0)$ is the second derivative of the signal over the two-photon (Raman) detuning at the extremum of the reference spectroscopic line (in our case, at the pseudoresonance position), and $W\sim\Gamma_s$ is the width of the detuning range, where S'' is approximately constant. The signal S is the transmitted laser

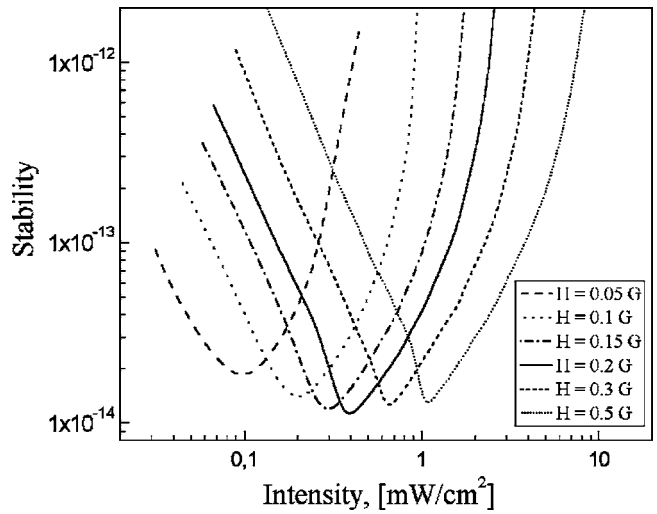

FIG. 7. Frequency standard stability (Allan deviation, dimensionless) for the integration time $\tau=1$ *s* versus laser field intensity for different magnetic fields.

power normalized to its value outside the CPT–resonance-induced structure but still within the Doppler profile of the D_1 line. The function $f(\Theta)$ is close to 1 in the optimal range of values of the cell optical thickness Θ $(0.5<\Theta<1)$. The standard stability estimation shows that short-term stability $\sigma_y \sim 10^{-14}/\sqrt{\tau}$ is achievable. Indeed, according to Eq. (7), the stability (at a given signal-to-noise ratio) is inversely proporstional to $|S''(0)|W \propto A/\Gamma_s$. The maximum value of the amplitude-to-width ratio is attained if most of the atoms contribute to the signal (that is easily achieved for the pseudoresonance excitation scheme) and the pseudoresonance width is minimized by a proper choice of the laser intensity. The combination of these two factors leads to an increase of A/Γ_s by an order of magnitude, compared to the conventional σ^+-excitation scheme, in the optimum range of laser intensities, as can be seen in Fig. 5. Therefore, the expected improvement of the standard performance is so significant.

We compared the results of our theoretical calculations to the experimental data of Ref. [22] and found a good agreement (see Fig. 8). Note that the parameters used in Ref. [22] are not optimum for the frequency standard design, since the laser intensity is higher than its optimum value, therefore the pseudoresonace is rather broad.

To conclude, we demonstrate theoretically the existence of a structure in a laser-light transmission spectrum under the CPT condition, a *pseudoresonance*, that is a narrow (having a width much less than the natural width of the excited state) absorption maximum between the two dark resonances involving $m=\pm 1$ sublevels of the ground state of an alkali atom, while CPT in the double Λ scheme based on $m=0$ is absent. The performance of an all-optical frequency standard using this effect for signal discrimination must be the same as that of a standard employing the "push-pull" technique [19,20]. However, a pseudoresonance-based standard is easier in both construction and handling and thus more suitable for application on board of a satellite or in other mobile instrument applications.

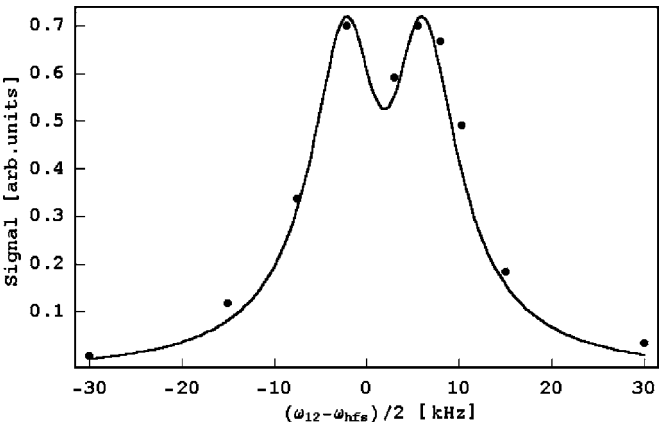

FIG. 8. Spectrum of the signal (the excess of the transmitted intensity over its background value far from the splitted dark resonance): our calculations (solid line) and data from Ref. [22] (points). The magnetic field $H=3$ G.

This research is supported by the INTAS-CNES, Project No. 03-53-5175, and by the Ministry of Education and Science of Russia, Project No. UR.01.01.287. We thank V. Yudin, D. Sarkisyan, C. Affolderbach, and E. Breschi for helpful discussions.

[1] J. Vanier and C. Audoin, *The Quantum Physics of Atomic Frequency Standards* (A. Hilger, Bristol, 1989).
[2] J. Vanier, Appl. Phys. B **81**, 421 (2005).
[3] N. Cyr, M. Tetu, and M. Breton, IEEE Trans. Instrum. Meas. **42**, 640 (1993).
[4] J. Kitching, S. Knappe, N. Vukičević, L. Hollberg, R. Wynands, and W. Weidmann, IEEE Trans. Instrum. Meas. **49**, 1313 (2000).
[5] J. Kitching, S. Knappe, and L. Hollberg, Appl. Phys. Lett. **81**, 553 (2002).
[6] M. Stähler, R. Wynands, S. Knappe, J. Kitching, L. Hollberg, A. Taichenachev, and V. Yudin, Opt. Lett. **27**, 1472 (2002).
[7] M. Merimaa, T. Lindvall, I. Tittonen, and E. Ikonen, J. Opt. Soc. Am. B **20**, 273 (2003).
[8] S. V. Kargapoltsev, J. Kitching, L. Hollberg, A. V. Taichenachev, V. L. Velichansky, and V. I. Yudin, Laser Phys. **1**, 495 (2004).
[9] G. Kazakov, I. Mazets, Yu. Rozhdestvensky, G. Mileti, J. Delporte, and B. Matisov, Eur. Phys. J. D **35**, 445 (2005).
[10] S. Knappe, L. Hollberg, and J. Kitching, Opt. Express **13**, 1249 (2005).
[11] B. D. Agap'ev, M. B. Gorny, B. G. Matisov and Yu. V. Rozhdestvensky, Phys. Usp. **36**, 763 (1993).
[12] E. Arimondo, in *Progress in Optics*, edited by E. Wolf (North-Holland, Amsterdam, 1996), 35, p. 257.
[13] S. Brandt, A. Nagel, R. Wynands, and D. Meschede, Phys. Rev. A **56**, R1063 (1997).
[14] D. V. Kosachev, B. G. Matisov and Yu. V. Rozhdestvensky, J. Phys. B **25**, 2473 (1992).
[15] D. A. Varshalovich, A. N. Moskalev, and V. K. Khersonsky, *Quantum Theory of Angular Momentum* (World Scientific, Singapore, 1988).
[16] V. Taichenachev, V. I. Yudin, V. L. Velichansky, and S. A. Zibrov, arXiv: eprint quant-ph/0503036.
[17] W. Maichen, F. Renzoni, I. Mazets, E. Korsunsky, and L. Windholz, Phys. Rev. A **53**, 3444 (1996).
[18] A. V. Taichenachev, V. I. Yudin, V. L. Velichansky, S. V. Kargapoltsev, R. Wynands, J. Kitchind, and L. Hollberg, JETP Lett. **80**, 236 (2004).
[19] Y.-Y. Jau, E. Miron, A. B. Post, N. N. Kuzma, and W. Happer, Phys. Rev. Lett. **93**, 160802 (2004).
[20] A. B. Post, Y.-Y. Jau, N. N. Kuzma, and W. Happer, Phys. Rev. A **72**, 033417 (2005).
[21] T. Zanon, S. Guerandel, E. de Clercq, D. Holleville, N. Dimarcq, and A. Clairon, Phys. Rev. Lett. **94**, 193002 (2005).
[22] S. A. Zibrov, Y. O. Dudin, V. L. Velichansky, A. V. Taichenachev, and V. I. Yudin, *Abstract Book of ICONO'05* (St. Pe-

tersburg, 2005), p. ISK8; V. A. Taichenachev, V. I. Yudin, V. L. Velichansky and S. A. Zibrov, arXiv: eprint quant-ph/0507090.

[23] S. Knappe, W. Kemp, C. Affolderbach, A. Nagel, and R. Wynands, Phys. Rev. A **61**, 012508 (1999).

[24] A. Nagel, S. Brandt, D. Meschede, and R. Wynands, Europhys. Lett. **48**, 385 (1999).

[25] F. Levi, A. Godone, and J. Vanier, IEEE Trans. Ultrason. Ferroelectr. Freq. Control **47**, 466 (2000).